論文 / 著書情報
Article / Book Information

Title	Prediction Method to Wind-Induced Peak Response of Building with Viscoelastic Dampers by Considering its Frequency Dependency
Authors	Daiki Sato, KAZUHIKO KASAI, TETSURO TAMURA
Citation	13th International Conference on Wind Engineering, , ,
Pub. date	2011, 7

Prediction Method to Wind-Induced Peak Response of Building with Viscoelastic Dampers by Considering its Frequency Dependency

Daiki Sato [a], Kazuhiko Kasai [b], Tetsuro Tamura [c]

[a] *Tokyo University of Science, Noda, Chiba, Japan, daiki-s@rs.noda.tus.ac.jp*
[b] *Tokyo Institute of Technology, Yokohama, Kanagawa, Japan, kasai@serc.titech.ac.jp*
[c] *Tokyo Institute of Technology, Yokohama, Kanagawa, Japan, tamura.t.ab@m.titech.ac.jp*

1 INTRODUCTION

In Japan, many high-rise buildings adopt the passive control devices, such as steel damper, oil damper, viscose damper, viscoelastic damper etc., to decrease the response of building. It has been recognized that the viscoelastic (VE) dampers have significant advantage over other types of dampers in controlling response of building against not only earthquake but also wind excitation. VE materials are typically made of polymers or glassy substances. Typical harmonic response based on the relation of force and deformation of VE damper is shown in Figure 1. It is commonly known that dynamic characteristics of VE damper are represented by $K'_d(\omega)$ and $K''_d(\omega)$, and these are depending on the frequency and temperature (Kasai et al. (1993), Sato et all (2007)). When a building with viscoelastic dampers is subjected to wind excitations, its dynamic properties such as vibration period and damping ratio can vary, depending on the frequency components of the excitation. This is due to frequency sensitivity of the viscoelastic damper, and contradicts the basis of the conventional spectral modal analysis method using the constant dynamic properties evaluated at resonant state of the building. This paper points out the need for considering frequency sensitivity of a building when it possesses velocity-dependent dampers such as viscoelastic dampers, and proposes for the first time a new spectral modal analysis method to predict the wind-induced response, considering the frequency sensitivity of the viscoelastic damper.

2 OUTLINE OF ANALYTICAL MODEL AND WIND FORCE

2.1 *Establishment of building model*

The 50-story building, with height H = 200 m, wide D = 50 m, depth D =50m, story height h = 4m and mass density ρ = 175 kg / m^3, is assumed for a model in this paper. 5-types of 1st mode's natural period T_1 (= 12, 10, 8, 6 and 4 sec) are prepared, and these are respectively called "6H, 5H, 4H, 3H and 2H frame". In this paper, these buildings are modeled by using single degree of freedom (SDOF) model as shown in Figure 2, where M = mass, K_f = frame stiffness, K_b = brace stiffness $K'_d(\omega)$ = damper storage stiffness, $K''_d(\omega)$ = damper loss stiffness. The damping ratio of frame ξ_0 is assumed 0 % in this study. The series connection of brace and damper is called as "added component" (Kasai et al (1998)).

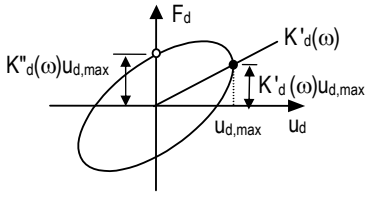

Figure 1. Hysteresis loop of VE damper

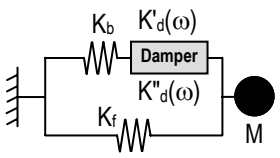

Figure 2. SDOF system

2.2 *Fluctuating wind force*

The wind velocity is set to the expected value with a 500-year return period as evaluated by A.I.J. recommendations. The power spectral density of along- and across- wind force is based on A. I. J. recommendation (a broken line in Figure 3), and, the time histories of 1st modal wind forces are shown in Figure 4(a), (b). The study described in this paper actually includes wind velocities and natural frequency areas in which problems of aero-mechanically unstable vibration cannot be ignored, but this is intended to show the suitability of the proposed technique under various conditions. This paper is based on the assumption that wind force characteristics do not change under structural vibration, and it does not deal with problems of aero-mechanically unstable vibration.

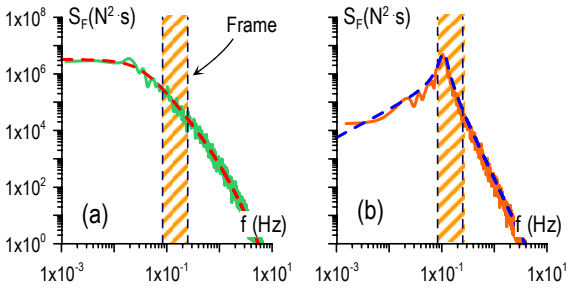

Figure 3. PSD of fluctuating wind force :
(a) Along direction, (b) Across direction

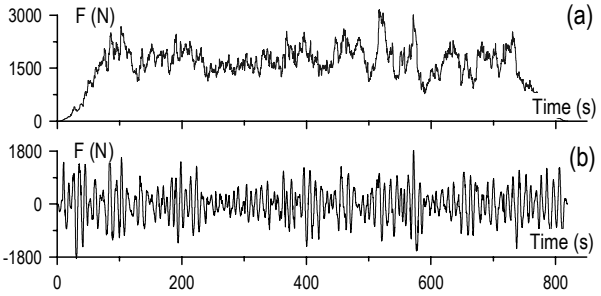

Figure 4. Time history of fluctuating wind force :
(a) Along direction, (b) Across direction

2.3 *Set up of VE damper and SDOF models*

In this paper, 25 (= 5x5) types of SDOF model having VE damper are totally used based on 5 types of dynamic property for both of structural model and VE damper. VE damper is modeled by using the fractional derivative (FD) model which can express frequency and temperature dependency of VE damper. In the typical harmonic response based on the relation of damper force F_d and deformation u_d as shown in Figure 1, $K'_d(\omega)$ and $K''_d(\omega)$ are depend on frequency ω ($= 2\pi f$). Then $K'_d(\omega)$, $K''_d(\omega)$ and loss factor $\eta_d(\omega)$ are expressed by Eq. (1a)-(c) (Kasai et al. (1993)), respectively.

$$K'_d(\omega) = G\frac{1+ab\omega^{2\alpha}+(a+b)\omega^{\alpha}\cos(\alpha\pi/2)}{1+a^2\omega^{2\alpha}+2a\omega^{\alpha}\cos(\alpha\pi/2)}\frac{A_s}{d} \tag{1a}$$

$$K''_d(\omega) = G\frac{(-a+b)\omega^{\alpha}\sin(\alpha\pi/2)}{1+a^2\omega^{2\alpha}+2a\omega^{\alpha}\cos(\alpha\pi/2)}\frac{A_s}{d} \tag{1b}$$

$$\eta_d(\omega) = \frac{K''_d(\omega)}{K'_d(\omega)} \tag{1c}$$

where, A_s = Laminations area of VE material, d = Thickness of VE material lamination, G, a, b and α are parameter of FD. In this paper, as the VE material, ISD 111 are adopted, these parameter are; G = 6.516 N/cm^2, a = 5.6 x 10^{-5}, b = 2.10, α = 0.558. As shown as Eq. (1), FD model can express the characteristic of VE damper by using ω, FD model is even more useful in the frequency domain.

The storage stiffness of added component $K'_a(\omega)$ and the loss stiffness of added component $K''_d(\omega)$ are calculated by Eq. (2a) and (2b), respectively.

$$K'_a(\omega) = \frac{\{(1+\eta_d^2(\omega))K'_d(\omega)+K_b\}K'_d(\omega)K_b}{(K'_d(\omega)+K_b)^2+(\eta_d(\omega)K'_d(\omega))^2} \tag{2a}$$

$$K''_a(\omega) = \frac{\eta_d(\omega)K'_d(\omega)K_b}{(K'_d(\omega)+K_b)^2+(\eta_d(\omega)K'_d(\omega))^2} \tag{2b}$$

The storage stiffness of system $K'(\omega)$ and the loss factor of system $\eta(\omega)$ are expressed by Eq. (3a) and (3b), respectively.

$$K'(\omega) = K_f + K'_a(\omega) \quad , \qquad \eta(\omega) = \frac{K''_a(\omega)}{K'(\omega)} \tag{3a, b}$$

The natural frequency of system $\omega'_n(\omega)$ and the damping ratio of system $\xi'_n(\omega)$ are calculated by Eq. (4a) and (4b), respectively.

$$\omega'_n(\omega) = \sqrt{\frac{K'(\omega)}{M}} \quad , \qquad \xi'_n(\omega) = \xi_0 + \frac{\eta(\omega)}{2}\cdot\frac{\omega'_n(\omega)}{\omega} \tag{4a, b}$$

As shown in Eq. (4), the natural frequency and damping ratio of system having VE damper are changed depend on the input frequency. The natural frequency ω_n, damping ratio of the resonance frequency ($\omega'_n(\omega) = \omega$) ξ_n are respectively expressed as follows;

$$\omega_n = \sqrt{\frac{K'(\omega_n)}{M}} \quad , \qquad \xi_n = \xi_0 + \frac{\eta(\omega_n)}{2} \tag{5a, b}$$

In this paper, 25-types of FD system are established as shown in Table 1.

Table 1. Model name and set up of model parameters

Model	K_f (N/m)	Damper	Brace	$\frac{K'_d(\omega_n)}{K_f}$	$\frac{K_b}{K_f}$	A_s/d (m)	f_n (Hz)	ξ_n
F-6H1	0.274	Hard	Hard	2.0	∞	6.156×10^{-6}	0.144	0.224
F-6H2		Soft		0.4		1.379×10^{-6}	0.099	0.087
F-6H3		Hard	Soft	2.0	3.0	6.406×10^{-6}	0.127	0.095
F-6H4		Soft		0.4		1.384×10^{-6}	0.097	0.069
F-6H5		Weak		0.077		2.759×10^{-7}	0.086	0.020
F-5H1	0.395	Hard	Hard	2.0	∞	8.366×10^{-6}	0.173	0.234
F-5H2		Soft		0.4		1.884×10^{-6}	0.118	0.091
F-5H3		Hard	Soft	2.0	3.0	8.717×10^{-6}	0.153	0.098
F-5H4		Soft		0.4		1.891×10^{-6}	0.117	0.072
F-5H5		Weak		0.073		3.571×10^{-7}	0.104	0.020
F-4H1	0.617	Hard	Hard	2.0	∞	1.213×10^{-5}	0.217	0.246
F-4H2		Soft		0.4		2.749×10^{-6}	0.148	0.097
F-4H3		Hard	Soft	2.0	3.0	1.265×10^{-5}	0.191	0.102
F-4H4		Soft		0.4		2.759×10^{-6}	0.146	0.076
F-4H5		Weak		0.068		4.896×10^{-7}	0.129	0.020
F-3H1	1.097	Hard	Hard	2.0	∞	1.948×10^{-5}	0.289	0.261
F-3H2		Soft		0.4		4.452×10^{-6}	0.197	0.103
F-3H3		Hard	Soft	2.0	3.0	2.035×10^{-5}	0.256	0.107
F-3H4		Soft		0.4		4.467×10^{-6}	0.195	0.081
F-3H5		Weak		0.065		7.454×10^{-7}	0.172	0.020
F-2H1	2.467	Hard	Hard	2.0	∞	3.759×10^{-5}	0.433	0.281
F-2H2		Soft		0.4		8.684×10^{-6}	0.296	0.112
F-2H3		Hard	Soft	2.0	3.0	3.932×10^{-5}	0.385	0.113
F-2H4		Soft		0.4		8.712×10^{-6}	0.293	0.088
F-2H5		Weak		0.057		1.311×10^{-6}	0.257	0.020

Figure 5 shows the comparison of frequency dependencies of K'_d, K''_d, f'_n (natural frequency) and ξ'_n(damping ratio) of F-3H1 system (Hard type damper) and F-3H2 (Soft type damper).

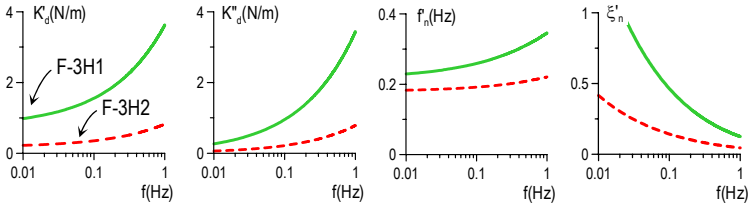

Figure 5. Frequency dependency of various dampers

3 PREDICTION OF DYNAMIC RESPONSES

3.1 *Predictive method of dynamic response considering frequency dependency*

This paper proposes a new predictive method for dynamic response based on the frequency domain analysis. It is assumed that the maximum response probability distribution can be predicted using the VE damper property. This proposed method is explained in the following paragraphs.

3.2 *Averaged values of deformation and force*

Figure 6(a)-(c) show loops of the damper force F_d and deformation u_d obtained by time history analysis subjected to the along wind force which have the non-zero mean component as shown in Figure 4(a). From Figure 6, it is recognized that the center of loop are drifted and the damper fore and deformation have the average value $F_{d,st}$ and $u_{d,st}$, respectively. The prediction method for $F_{d,st}$ and $u_{d,st}$, are shown as follows;
From Eq. (1a) and (1b), the static storage stiffness of damper $K'_{d,st}$ and the static loss stiffness of damper $K''_{d,st}$ are calculated by Eq. (6a), (6b), respectively.

$$K'_{d,st} = \lim_{\omega \to 0} K'_d(\omega) = G\frac{A_s}{d} \quad , \qquad K''_{d,st} = \lim_{\omega \to 0} K''_d(\omega) = 0 \tag{6a, b}$$

The static stiffness of added component $K'_{a,st}$ and the loss stiffness of added component $K''_{d,st}$ are calculated by Eq. (7a) and (7b), respectively.

$$K'_{a,st} = \frac{K_b \cdot K'_{d,st}}{K_b + K'_{d,st}} \quad , \qquad K''_{a,st} = 0 \tag{7a, b}$$

The static stiffness of system K'_{st} can be expressed by Eq. (8), and K'_{st} is not depended on the input frequency.

$$K'_{st} = K_f + K'_{a,st} \tag{8}$$

The average displacement of system x_{st} is calculated by using the average wind force F_{st} as following equation.

$$x_{st} = K'_{st} / F_{st} \tag{9}$$

By using the average displacement of system x_{st}, the average deformation of damper $u_{d,st}$ and force $F_{d,st}$ are obtained by Eq. (10a) and (10b), respectively.

$$u_{d,st} = \frac{1}{1 + K'_{d,st}/K_b} x_{st} \ , \quad F_{d,st} = K'_{d,st} \cdot u_{d,st} \tag{10a,b}$$

The predicted $u_{d,st}$ and $F_{d,st}$ are shown in Figure 6 as the cross symbol. It can be confirmed that the present predictive method has excellent accuracy in comparison with time domain analysis.

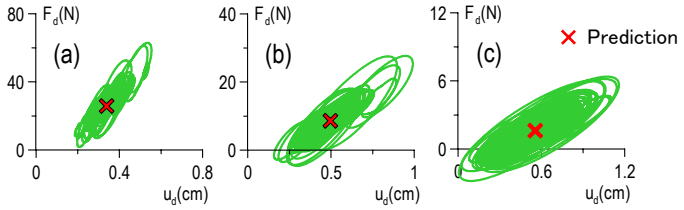

Figure 6. Prediction of average deformation and force of damper :
(a) F-3H1, (b) F-3H2, (c) F-3H5

3.3 *Power spectral density of dynamic responses*

The power spectral density (PSD) of fluctuating displacement $S_D(\omega)$, velocity $S_V(\omega)$ and acceleration $S_V(\omega)$, which can consider the frequency dependency of VE damper, are give by following equations.

$$S_D(\omega) = |H(\omega)|^2 S_F(\omega),\quad S_V(\omega) = |\dot{H}(\omega)|^2 S_F(\omega),\quad S_A(\omega) = |\ddot{H}(\omega)|^2 S_F(\omega) \qquad (11a\text{-}c)$$

where $H(\omega)$ is the transfer function of the system having VE damper considering the frequency dependency, and it is calculated by using $K'_a(\omega)$ and $K''_d(\omega)$ (Eq. (2)) as follows;

$$H(\omega) = \frac{1}{1-\left(\dfrac{\omega}{\omega_0}\right)^2 + \dfrac{K'_a(\omega)}{K_f} + i\left(2\xi_0 \dfrac{\omega}{\omega_0} + \dfrac{K''_a(\omega)}{K_f}\right)} \cdot \frac{1}{K_f} \qquad (12a)$$

$$\dot{H}(\omega) = i\omega H(\omega),\quad \ddot{H}(\omega) = -\omega^2 H(\omega) \qquad (12b, c)$$

The standard deviation of displacement σ_D, velocity σ_V and acceleration σ_A are calculated by Eq. (13).

$$\sigma_D = \sqrt{\int_0^\infty S_D(\omega)d\omega}\ ,\quad \sigma_V = \sqrt{\int_0^\infty S_V(\omega)d\omega}\ ,\quad \sigma_A = \sqrt{\int_0^\infty S_A(\omega)d\omega} \qquad (13a\text{-}c)$$

Figure 7(a), (b) show respectively the comparison of PSD of responses predicted by the time history analysis and the proposed method (Eq. (11)) in along and across wind directions. This proposed predictive method utilizes the transfer function which can consider the frequency dependency of VE damper. The prediction results agree well with the results by time domain analysis. The prediction results agree well with the results by time history analysis. In Figure 7, ε is expressed by Eq. (14), and represents the characteristics of PSD.

$$\varepsilon = \sqrt{1 - \frac{\sigma_V^4}{\sigma_D^2 \sigma_A^2}} \qquad (14)$$

3.4 *Maximum response probability distribution*

In this session, the maximum response probability distribution considering the frequency dependency of VE damper is discussed. In this paper, the maximum displacement probability distribution $p_D(\zeta)$ is proposed as follows;

$$p_D(\zeta) = p_1(\zeta) \Big/ \int_0^\infty p_1(\zeta)d\zeta \qquad (\zeta > 0) \qquad (15)$$

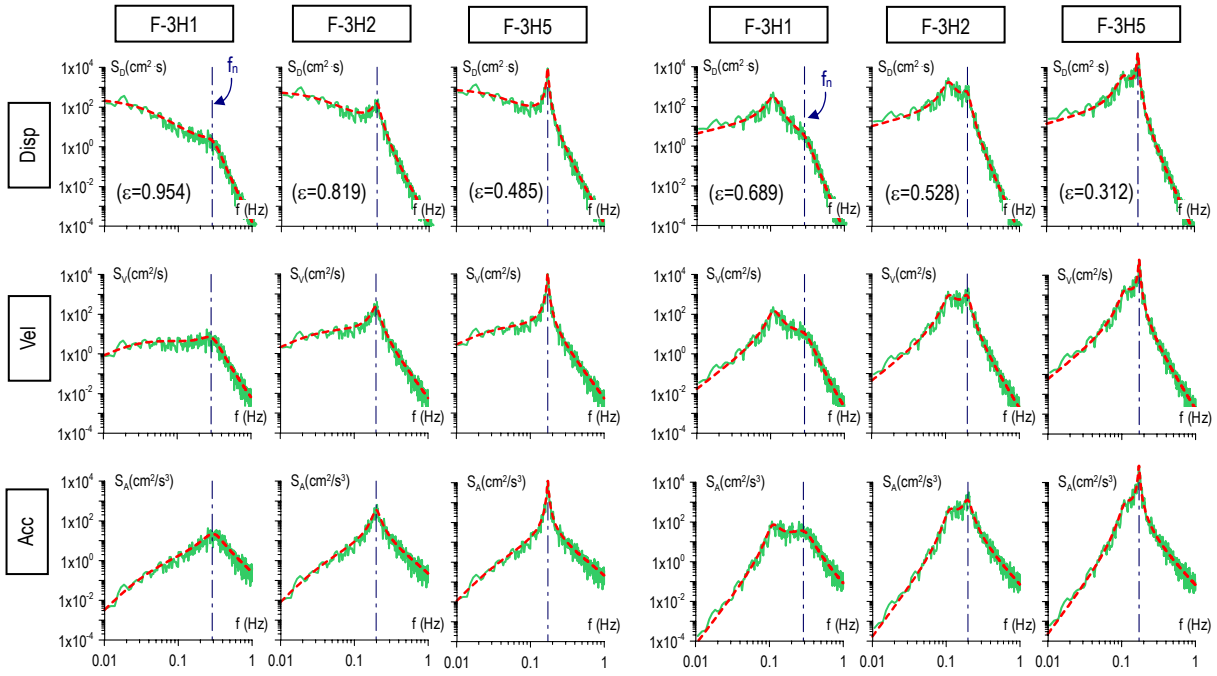

(a) Along direction (b) Across direction

Figure 7. Comparison of response PSD — Time history — Prediction

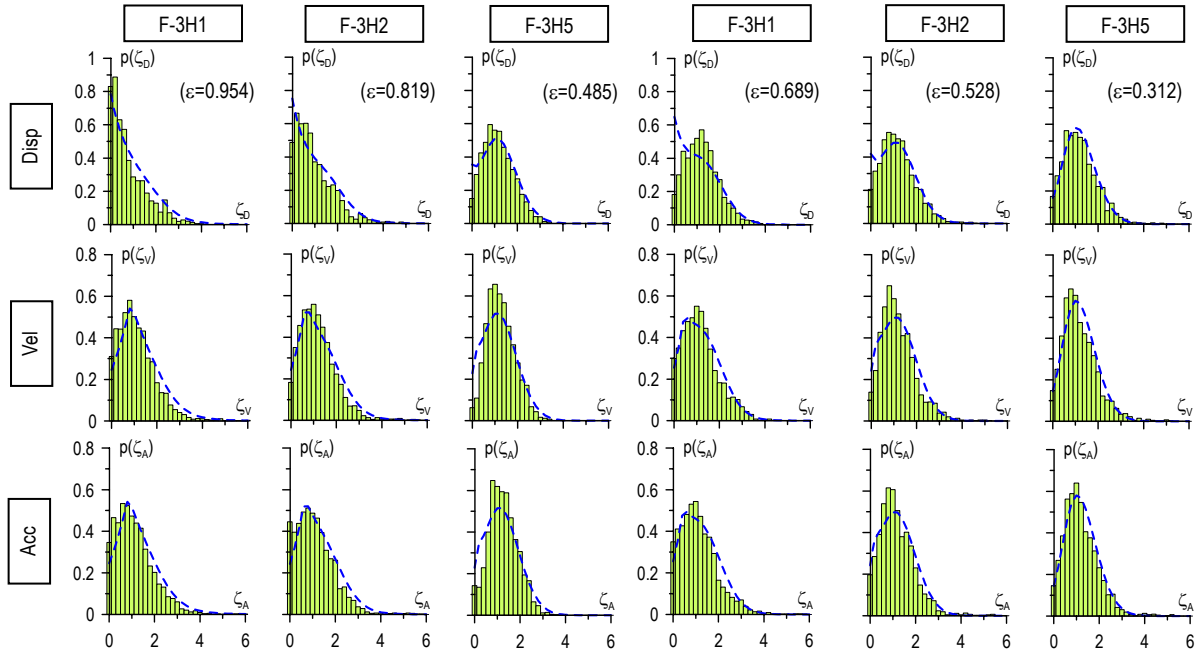

(a) Along direction (b) Across direction

Figure 8. Comparison of maximum response probability distribution — Time history — Prediction

where;

$$p_1(\zeta) = p(\zeta') + \beta(\varepsilon - 0.1)\exp(-\zeta'/\varepsilon) \tag{16}$$

here, $p(\zeta)$ represents the probability density function (Cartwright and Longuet (1956)).

$$p(\zeta)=\frac{1}{\sqrt{2\pi}}\left[\varepsilon\exp\left(-\frac{\zeta^2}{2\varepsilon^2}\right)+\alpha_p\exp\left(-\frac{\zeta^2}{2}\right)\cdot\int_{-\infty}^{\frac{\alpha_p}{\varepsilon}}\exp\left(-\frac{z^2}{2}\right)dz\right] \tag{17}$$

$$\alpha_p=\zeta\sqrt{1-\varepsilon^2}\ ,\quad \zeta'=\zeta-\beta(\varepsilon-0.1)\ ,\quad \beta=0.5\cos(1-\pi\varepsilon) \tag{18a - c}$$

$$\int_{-\infty}^{\frac{\alpha_p}{\varepsilon}}\exp\left(-\frac{z^2}{2}\right)dz=\frac{\sqrt{2\pi}}{2}\left\{\mathrm{erf}\left(\frac{\alpha_p}{\varepsilon\sqrt{2}}\right)+1\right\} \tag{19}$$

where, in Eq. (19), erf( ) is error function.
The maximum velocity probability distribution $p_V(\zeta)$ and acceleration probability distribution $p_A(\zeta)$ are suggested as following equations. From the time history analysis results as shown in Figure 9, it can be assumed that $p_A(\zeta)$ are same as $p_V(\zeta)$.

$$p_V(\zeta)=p_A(\zeta)=p_2(\zeta)\Big/\int_0^{\infty}p_2(\zeta)d\zeta \tag{20}$$

where;

$$p_2(\zeta)=p(\zeta')+\beta(\varepsilon-0.1)\exp\left(-|\zeta'|/(\varepsilon-0.1)\right) \tag{21}$$

Figures 8(a), (b), respectively, show the comparison of maximum response probability distribution in along and across wind directions predicted by the time history analysis and the proposed frequency domain analysis. By using this method, the maximum response probabilities can be estimated with a high accuracy even if the structure has not only the frequency sensitivity but also large damping ratio.

4 VERIFICATION OF PROPOSED PREDICTIVE METHOD

The probability density function of displacement $P_{D,max}(\zeta)$, velocity $P_{V,max}(\zeta)$ and acceleration $P_{A,max}(\zeta)$ are expressed as following equations.

$$p_{D,\max}(\zeta)=N_D\left[1-q_D(\zeta)\right]^{N_D-1}p_D(\zeta)\ ,\quad q_D(\zeta)=\int_{\zeta}^{\infty}p_D(\zeta)d\zeta \tag{22a, b}$$

$$p_{V,\max}(\zeta)=N_V\left[1-q_V(\zeta)\right]^{N_V-1}p_V(\zeta)=p_{A,\max}(\zeta)\ ,\quad q_V(\zeta)=\int_{\zeta}^{\infty}p_V(\zeta)d\zeta \tag{23a, b}$$

where, N_D and N_V can be calculated by Eq. (24a), (24b), respectively.

$$N_D=\nu_{0,D}^{+}T_a=\frac{1}{2\pi}\left(\frac{\sigma_V}{\sigma_D}\right)T_a\ ,\quad N_V=\nu_{0,V}^{+}T_a=\frac{1}{2\pi}\left(\frac{\sigma_A}{\sigma_V}\right)T_a \tag{24a, b}$$

where, T_a is the duration time, $\nu_{0,D}^{+}$ and $\nu_{0,V}^{+}$ represent zero crossing number of the displacement and velocity and given by following equations, respectively.

$$\nu_{0,D}^{+}=\frac{1}{2\pi}\left(\frac{\sigma_V}{\sigma_D}\right),\quad \nu_{0,V}^{+}=\frac{1}{2\pi}\left(\frac{\sigma_A}{\sigma_V}\right) \tag{25a, b}$$

The peak factor of displacement g_D, velocity g_V are obtained by Eq. (26a), (26b), respectively.

$$g_D=\int_{-\infty}^{\infty}\zeta\,p_{D,\max}(\zeta)d\zeta\ ,\quad g_V=\int_{-\infty}^{\infty}\zeta\,p_{V,\max}(\zeta)d\zeta \tag{26a, b}$$

The maximum displacement of system in the along wind direction is calculated by Eq. (27a), the maximum velocity and acceleration are given by Eq. (27b), (27c), respectively.

$$x_{\max} = x_{st} + \sigma_D g_D \ , \quad \dot{x}_{\max} = \sigma_V g_V \ , \quad \ddot{x}_{\max} = \sigma_A g_A \qquad (27a - c)$$

Figures 9 and 10 demonstrate respectively the error estimations of predictive responses in along and across wind directions. This prediction method can estimate maximum displacement within 20% accuracy. However, the predictions of maximum velocity and acceleration need to be improved.

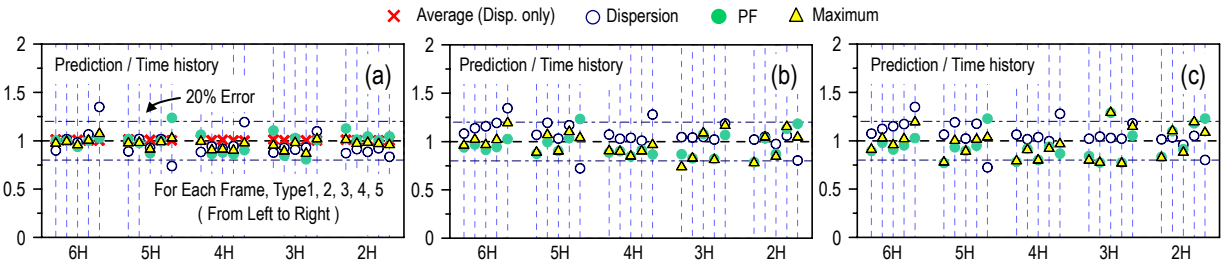

Figure 9. Error estimation in along direction : (a) Displacement, (b) Velocity, (c) Acceleration

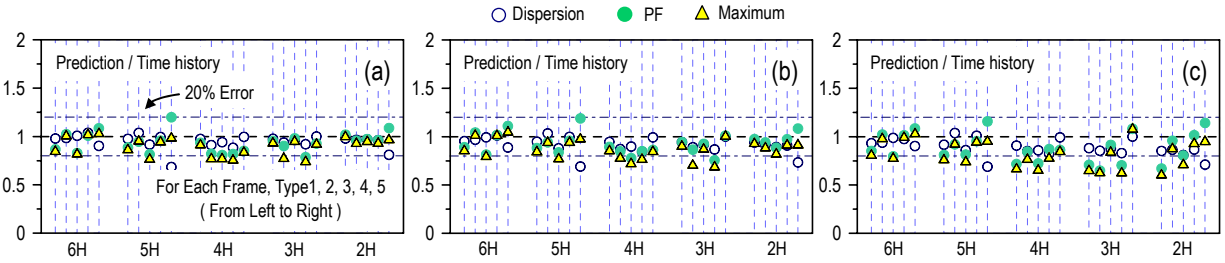

Figure 10. Error estimation in across direction : (a) Displacement, (b) Velocity, (c) Acceleration

5 CONCLUSIONS

This paper proposes the new predictive method to wind-induced peak response of building with viscoelastic (VE) dampers by considering its frequency dependency. Good accuracy of this predictive method is demonstrated by comparing with the results by time history analysis. This predictive method can be used effectively for design of the building having VE damper.

References:

Kasai, K., Munshi, J.A., Lai, M.-L, and Maison, B.F., 1993, Viscoelastic Damper Hysteresis Model, Theory, Experiment, and Application, ATC17-1 Seminar Applied Technology Council, Vol1.2, 521-532.

Kasai, K., Fu, Y. and Watanabe A., 1998, Passive Control Systems for Seismic Damage Mitigation, Journal of Structural Engineering, ACSE, Vol.124, No5, May, 501-512

Sato, D., Kasai, K., and Tamura, T., 2007, Properties of Viscoelastic Damper under Wind Load and Analytical Method Considering Heat Conduction & Transfer, 12th ICWE, 1263-1270

Architectural Institute of Japan, Recommendations of Loads on Buildings, 2004

Cartwright, D.E. and Longuet-Higgins, M.S., 1956, The Statistical Distribution of the Maxima of a Random Function, Proceedings of the Royal Society of London, Series A. Vol.237, pp.212-232